

Economic and environmental analysis of a novel rural house heating and cooling system using a solar-assisted vapour injection heat pump

 The corrections made in this section will be reviewed and approved by a journal production editor.

[Instruction: * Corresponding author (Xudong Zhao) . Tel.: +44-01482466684, Email:

xudong.zhao@hull.ac.uk ** Corresponding author (Jing Li). Tel.: +44-01482463611, Email:

jing.li@hull.ac.uk] Yi Fan Writing - original draft Formal analysis Methodology Investigation ^a, Xudong

Zhao Funding acquisition Conceptualization Supervision ^a, Jing Li Project administration Conceptualization

Supervision ^a, Guiqiang Li Resources ^a, Steve Myers Writing - review & editing ^a, Yuanda Cheng Software

^b, Ali Badiei Writing - review & editing ^a, Min Yu Data curation ^a, Yousef Golizadeh Akhlaghi Resources ^a,

Samson Shittu Validation ^a, Xiaoli Ma Writing - review & editing ^a

^aResearch Centre for Sustainable Energy Technologies, University of Hull, Hull HU6 7RX, UK

^bCollege of Environmental Science and Engineering, Taiyuan University of Technology, 030024, China

Abstract

An efficient low-carbon system is proposed to meet the heating and cooling demands of rural houses in cold regions. Mini-channel solar panels incorporating a novel multiple-throughout-flowing loop are used for heat collection, whilst a vapour injection air source heat pump (VI-ASHP) is innovatively combined with an underfloor heating and cooling system. To demonstrate the system, a multiple-throughout-flowing mini-channel solar thermal panel array of 36 m² and a VI-ASHP of 40 kW heating capacity have been built and tested. Subsequently, mathematical models of the solar-assisted VI-ASHP system are established and compared with the experimental data. Based on the validated models, the energetic, economic and environmental performance is investigated under the typical weather conditions for a northern Chinese city (Taiyuan). The results indicate that, for a common rural house employing the proposed novel system, the proportion of the annual heat requirement, cooling load and hot water heating energy provided by solar thermal energy, photovoltaic energy and electricity from the power grid is 74.6%, 6.9%, and 18.5% respectively, thus giving a total energy supply proportion of 81.5% from solar energy. In addition, compared with a coal-powered system, our system has a cost payback period of 6.52 years and a life-cycle net cost saving of 56328.4RMB, thus the proposed system provides a greater economic performance. Furthermore, it can save 5 tons of anthracite coal and reduce carbon emissions by 12.1 tons annually. The proposed solar-assisted VI-

Keywords: Solar energy; Mini-channel collector; Vapour injection air source heat pump; Underfloor heating and cooling; Carbon emission; Payback period

Nomenclature

A_{st}	Area of the solar thermal panels, m^2 ;
A_e	Area of a single PV panel, m^2 ;
b	Index of the air permeability of outer doors and windows;
C_{cIC}	Solar radiation cooling load factor;
C_z	Comprehensive shielding coefficient of outer window;
C_w	Correction factor of the outer shielding device;
C_n	Correction factor of the inner shielding device;
C_s	Correction factor of the window glass;
C_{people}	Number of people;
C_{PT}	Cost of the solar thermal panel, RMB;
C_{PV}	Cost of the PV panel, RMB);
C_{HSEU}	Cost of the heat storage and exchange unit, RMB;
C_{HP}	Cost of the heat pump, RMB;
C_{ADD}	Additional cost of the system, RMB;
C_p	Specific heat capacity, $J/(kg \cdot K)$;
COP	Coefficient of performance for winter heating;
C_c	Initial capital cost, RMB;
C_{RE}	Renewable Heat Incentive (RHI) scheme, RMB;
C_o	Cost of operation, RMB;
C_m	Cost of maintenance, RMB;
CS	Life-cycle net cost saving, RMB;
$D_{J,max}$	Maximum index of the local solar radiation passing a glass in summer, W/m^2 ;
EER	Energy efficiency ratio for summer cooling;
F_c	Outer window area, m^2 ;
h_t	Heat transfer rate of the served house envelope, $W/(m^2 \cdot K)$;
I	Solar thermal radiation, kW/m^2 ;
L_{air}	Cold air infiltration volume per hour, m^3/h ;
L_0	Cold air infiltration volume per hour per meter, $m^3/(h \cdot m)$;
l_0	Length of the outer windows and doors, m;
\dot{m}	Mass flow rate of the working fluid (kg/s);
$m_{c.c}$	Consumed standard coal by a coal-powered heating system, kg;
m_p	Air contaminations generated by systems, kg;
m_{pu}	Air contaminations generated by using per unit fuel, kg;
N	Number of the PV panels;
$NOTC$	Nominal operating cell temperature;

PP	Cost payback period;
P_{wp}	Power of water pump, kW;
$Q_{h.l.am}$	Heating load of house envelops, kWh;
$Q_{h.l.wind}$	Heating load of house cold air infiltration, kWh;
$Q_{c.l}$	Cooling load of the served house, kWh;
$Q_{c.l.am}$	Cooling load of house envelops, kWh;
$Q_{c.l.solar}$	Cooling load generated by solar radiation, kWh;
$Q_{c.l.people}$	Cooling load generated by body heat dissipation, kWh;
$Q_{h.l}$	Heating load of the served house, kWh;
Q_{st}	Collected solar thermal energy, kWh;
Q_{people}	Maximum cooling load generated by one person, W/person;
Q_{se}	Electricity generation by PV panels, kWh;
$Q_{ec.wh}$	Electricity consumed by heat pump for winter heating, kWh;
$Q_{ec.sc}$	Electricity consumed by heat pump for summer cooling, kWh;
Q_{hp}	Heating capacity of the heat pump, kWh;
Q_{cp}	Cooling capacity of the heat pump, kWh;
Q_{hd}	Heat deficit provided by heat pump, kWh;
$Q_{ec.wp}$	Electricity consumed by water pump, kWh;
q_c	Calorific value generated by per ton of standard coal;
S_e	Envelopes area, m^2 ;
$T_{r.h.l}$	Setting room temperature during heating season, $^{\circ}C$;
$T_{r.c.l}$	Setting room temperature during cooling season, $^{\circ}C$;
T_{am}	Ambient temperature, $^{\circ}C$;
T_{in}	Inlet temperature of individual solar thermal panel, $^{\circ}C$;
T_c	Working temperature of the panel, $^{\circ}C$;
T_{rc}	Reference temperature, 25 $^{\circ}C$;
ΔT_{aw}	Temperature difference between T_a and T_{w2} , $^{\circ}C$;
t_i	Temperature of the i node along the multiple-throughout-flowing panel array, $^{\circ}C$;
T_{w2}	Temperature of heating water, $^{\circ}C$;
v_0	Local average wind velocity in the winter, m/s;
W_{ec}	Power of the heat pump, kW;
α_{air}	coefficient of air permeability of outer doors and windows, $m^3/(m \cdot h \cdot Pa)$;
$\alpha_{h.l}$	Coefficient of orientation correction of the house envelops;
β_{PV}	Temperature coefficient;
$\tau_{h.l}$	Heating time, h;
$\tau_{c.l}$	Cooling time, h;
η_{ot}	Overall solar thermal efficiency of the mini-channel solar thermal panel-array;
η_{it}	solar thermal efficiency of a individual mini-channel solar thermal panel;
η_i	Solar thermal efficiency of the i solar thermal panel;
η_{rc}	Initial electrical efficiency at reference temperature, 25 $^{\circ}C$;
η_e	Photoelectric efficiency;

η_c	Efficiency of a coal-powered heating system;
τ_{st}	Solar collectors operation time, h;
τ_{wy}	Electricity generation time, h;
τ_{wp}	Operation time of the water pump, h;
ρ	Density, kg/m ³ ;
\emptyset	Clustering coefficient;

Subscripts

<i>sp</i>	Solar-powered system;
<i>c</i>	Coal-powered system;
<i>.w</i>	West facing;
<i>.e</i>	East facing;
<i>.s</i>	South facing;
<i>.n</i>	North facing;
<i>air</i>	Air;
<i>wf</i>	Working fluid;

1 Introduction

Energy consumption for space heating [1] and hot water [2] accounts for the majority of total building energy consumption in the north of China, and so far most of the rural houses have been using coal as the main energy source for cooking, space heating and hot water supplying. This has caused severe fossil fuel shortage and environmental pollution including a high level of harmful dust, PM2.5 concentration, greenhouse gas, CO₂ and harmful gases, i.e. SO₂ and NO_x [3]. The summer in most areas of northern China is hot and an ambient temperature above 30 °C is common. The demand for cooling in rural houses is growing with the improvements in people's living standards.

The development of solar technology during recent years has brought revolutionary advances to existing energy systems. Recently, the mini-channel solar thermal collector has been widely investigated. The mini-channel is an aluminium tube with a size of about 1 – 4 mm, which has been used to improve the performance of solar thermal collectors in recent years [4]. Compared to the conventional copper tube flat-plate panels, the smaller interior space of the mini-channels provides a superior performance on many aspects, i.e. higher heat transfer rate and flow velocity, enhanced solar efficiencies [5], lower convective heat loss and lower cost [6]. Li et al. conducted a simulative and experimental study on mini-channel heat pipe under different evaporator temperatures and tilt angles. The useful results were achieved for the system design, optimization, and installation [7]. Deng et al. studied the performance of a solar-powered hot water system with a mini-channel-heat-pipe array, showing that the annual average system efficiency was 58.29% [8]. As a result, employing a mini-channel solar thermal panel could improve the amount of heat collection and reduce the cost of the system [9]. Notably, there are three desirable characteristics of northern Chinese rural houses for the utilization of solar energy systems: (1) a large flat roof area for the solar panels installation [10]; (2) rich solar resources throughout the year [11]; and (3) high residential density of large energy demand and low network energy loss. As a result, the potential to utilize solar energy systems in rural areas is larger than in urban buildings. Furthermore, solar energy systems can significantly reduce the local air pollution.

In addition to the solar technology, the air source heat pump (ASHP) is recognized as an energy-saving approach and has been widely used for space heating and hot water supply in central and northern China [12]. However, with a single-stage compression cycle, the conventional ASHP cannot operate efficiently and steadily in low ambient temperatures [13], due to the low coefficient of performance (COP) and frost formation [14]. The drawbacks of conventional ASHPs have been investigated by many researchers [15,16]. To further address the problems associated with conventional ASHPs, the vapour injection (VI) technique is attracting increasing interest [17]. Wang et al. investigated a two-stage air-source heat pump with a flash tank cycle to optimise the intermediate pressure with a real-time optimization method that can retain the use of saturated vapor for the injection line [18]. The capacity and COP of the VI compressor are significantly higher compared to that of the conventional compressors, especially at extremely low ambient temperatures [19]. The reason for the performance improvement lies in the enthalpy difference across the evaporator, which is larger with the two-stage expansion [19]. In addition to the remarkable improvement in heating mode, VI also provides significant improvements and enhanced cooling capacity when applied to air conditioning systems [20]. The advantages of VI technique have been validated by a commercialised system, elsewhere [21].

When it comes to the integration of the solar and heat pump systems in houses, hydronic radiant heating and cooling systems have become quite mature [22]. The underfloor heating system can be an efficient alternative to other more common forms of heating [23]. It conserves living and working space as it is integrated into the building structure. Furthermore, it can reduce the energy needed for seasonal heating by 18% [24] and improve the thermal comfort conditions inside the building [25]. Due to a lower exergy destruction by higher supply temperatures, radiant cooling systems enable more gains [26]. In particular, using the radiant cooling systems in northern China can efficiently reduce the condensation on floor surfaces thanks to the low air humidity.

So far, very few studies on the hybrid solar and VI-ASHP systems have been reported. Chen et al. [27] proposed a new direct-expansion solar-assisted VI-ASHP cycle with a sub-cooler for a water heater. The results showed that the new technology provided an average of 14.6% and 42.9% improvement in the COP and capacity, compared with the conventional technology. Lu et al. [28] investigated the solar photovoltaic/thermal heat pump system with VI cycle. According to the results, the average COP_{th} and COP_{PVT} of the PVT-VIASHP system were 3.27 and 3.45, respectively.

However, previous studies on solar-assisted VI-ASHP were focused on the heating performance, and the tests were conducted on a laboratory scale. The technology demonstration has yet to be implemented. To meet the heating and cooling demands and reduce carbon emissions in rural houses in northern China, this paper proposes a novel solar-assisted heat pump system. Mini-channel solar collectors are used for heat collection and a vapour injection air source heat pump (VI-ASHP) is incorporated with an underfloor heating and cooling system. Moreover, PV panels are employed to provide electricity for the system. An economic and environmental investigation of the system is carried out. The novelty and contributions of the current work include:

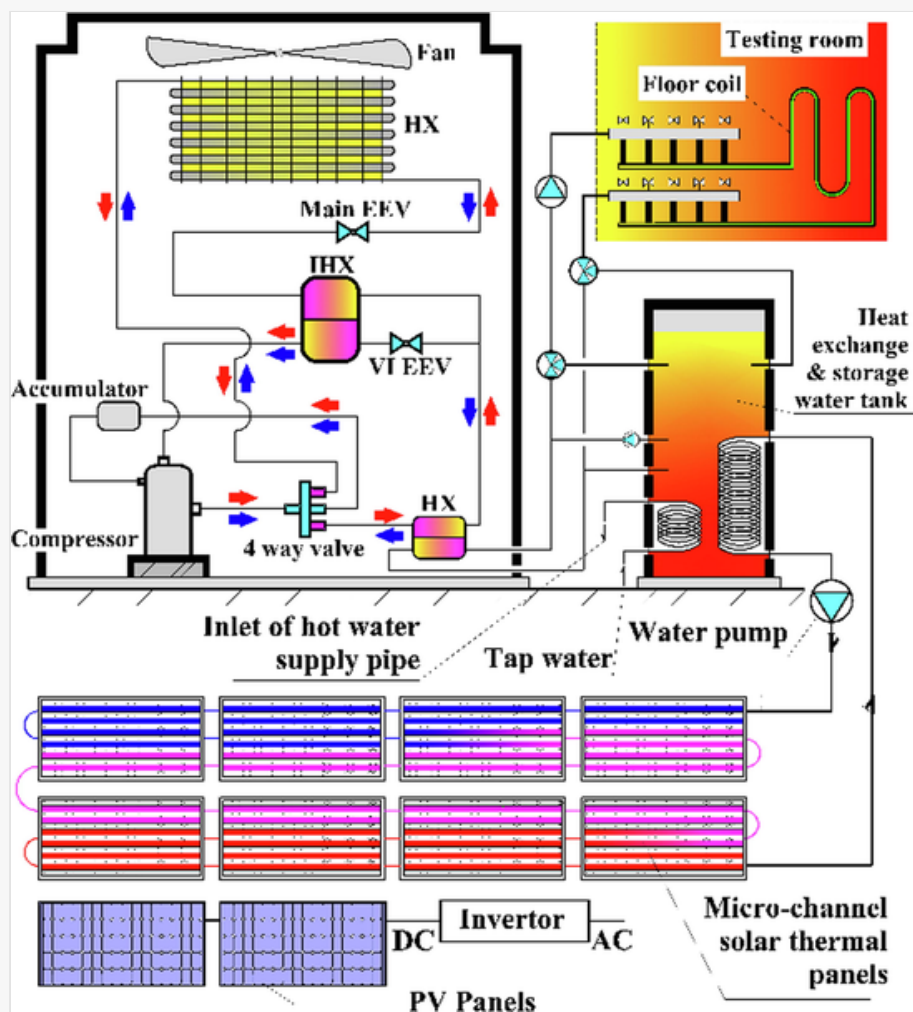
- (1) It is the first time that mini-channel solar thermal panels have been combined with VI-ASHP, thus forming a novel solar-assisted VI-ASHP system. The proposed system is further incorporated with an underfloor heating and cooling unit to satisfy the residents' annual energy needs.
- (2) Not only the heat supply but also cooling performance and hot water supply of the system are simulated. VI-ASHP is attracting increasing interest in cold regions and studies on its performance in heating mode have been conducted. Its potential in underfloor cooling applications is rarely explored.
- (3) The demonstrative system is constructed and presented. 18 mini-channel solar panels with a

combined aperture area of 36 m² have been demonstrated and tested in the multiple-throughout-flowing connection method in northern China. Unlike conventional solar panels, which are connected either in series or in parallel and normally have one inlet and outlet, the panels here are connected in a novel multiple-throughout-flowing manner. In addition, the demonstrative VI-ASHP system of heating capacity of about 40 kW has also been developed in northern China, providing valuable experimental results.

2 System description

The schematic of the novel solar-assisted VI-ASHP space heating, cooling and hot water supply system is shown in Fig. 1. The system is designed to meet the energy demand of a 100 m² rural house in northern China. It is comprised of: (1) one multiple-throughout-flowing panel array with 8 mini-channel solar thermal panels; (2) a dedicated PV panel array which can earn a profit, thus reducing the operational cost and fossil fuel consumption; (3) a heat storage and exchange unit (HSEU) that stores excess solar heat when the collected heat is greater than the heat demand of the building, and discharges heat into the served house when needed; (4) a VI-ASHP as a heating device in winter to provide space heating when solar energy and stored energy cannot meet the heat demand, and as a cooling device in summer.

Fig. 1



Schematic of the mini-channel solar-powered VI-ASHP system.

The technical specifications of the system's individual components are presented in Table 1. The control scheme of the proposed system for the heating process is divided into three main steps: (1) When the solar loop fluid

temperature is higher than the water tank temperature, the water pump on the solar loop operates to transfer the collected heat, as shown in Fig. 2(a); (2) When the water tank temperature is higher than 40 °C, it can facilitate space heating, as shown in Fig. 2(b); (3) When the solar energy and the stored energy are not enough for space heating, the VI-ASHP operates to meet the heating load, which is shown in Fig. 2(c);

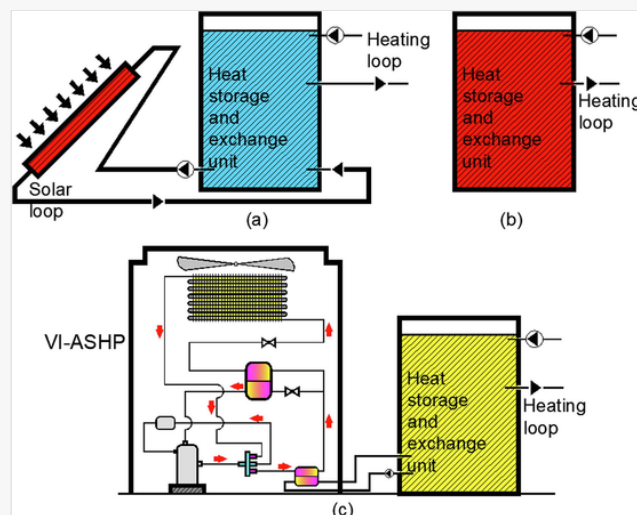
Table 1

i The table layout displayed in this section is not how it will appear in the final version. The representation below is solely for providing corrections to the table. To preview the actual presentation of the table, please view the Proof.

Technical specifications for the components of the system.

Name	Size	Number	Technical index
PV panels	1 m × 2 m	4	Crystalline silicon solar cells
Solar thermal panels	1 m × 2 m	8	Mini-channels
VI-ASHP	1.5 m × 0.5 m × 1 m	1	Nominal condition heating output: 12000 W
Heat storage and exchange unit	Diameter: 1.19 m, Height: 1.38 m	1	Volume: 1.5 m ³
Under floor coil	Diameter: 16 mm	300 m	Material: PE-X

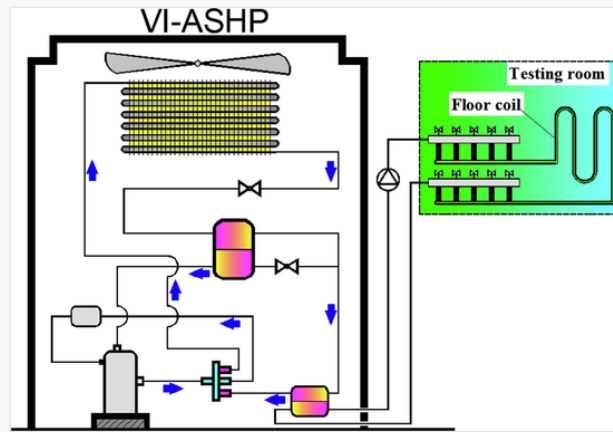
Fig. 2



Heating process of the proposed system.

The processes for domestic hot water supply and cooling are relatively simple. For domestic hot water, when the water tank temperature rises to 50 °C, hot water can be supplied by opening the hot water tap directly. For the cooling process, the VI-ASHP can exchange the circular route between the evaporator and condenser by using a four-way reversing valve and hence supply cooling directly through the under-floor coil, as shown in Fig. 3.

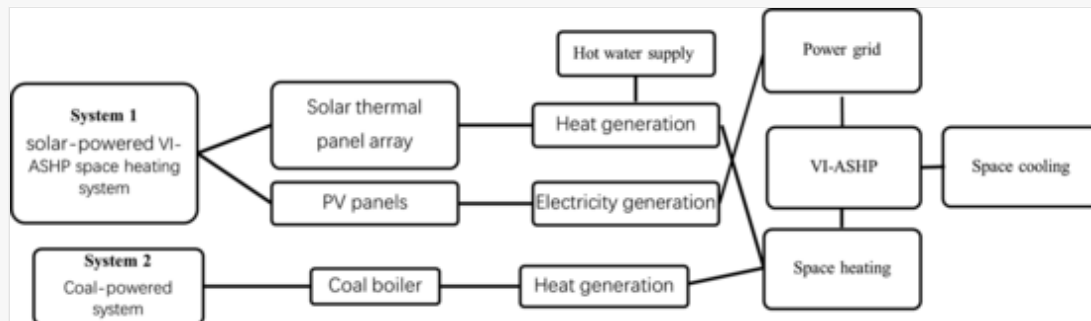
Fig. 3



Cooling process of the proposed system.

Consequently, the proposed system can provide space heating, cooling and hot water with low electricity consumption and reduced electricity cost. Several indexes, including the systems energy consumption, systems cost, cost payback period and contaminant generation are employed to evaluate the performance of the system relative to coal-powered systems. The heating, cooling and hot water supply processes of the two systems are shown in Fig. 4. To provide a reference point for comparison, the performance of a conventional coal-based system is also analysed.

Fig. 4



The heat generation processes of the systems.

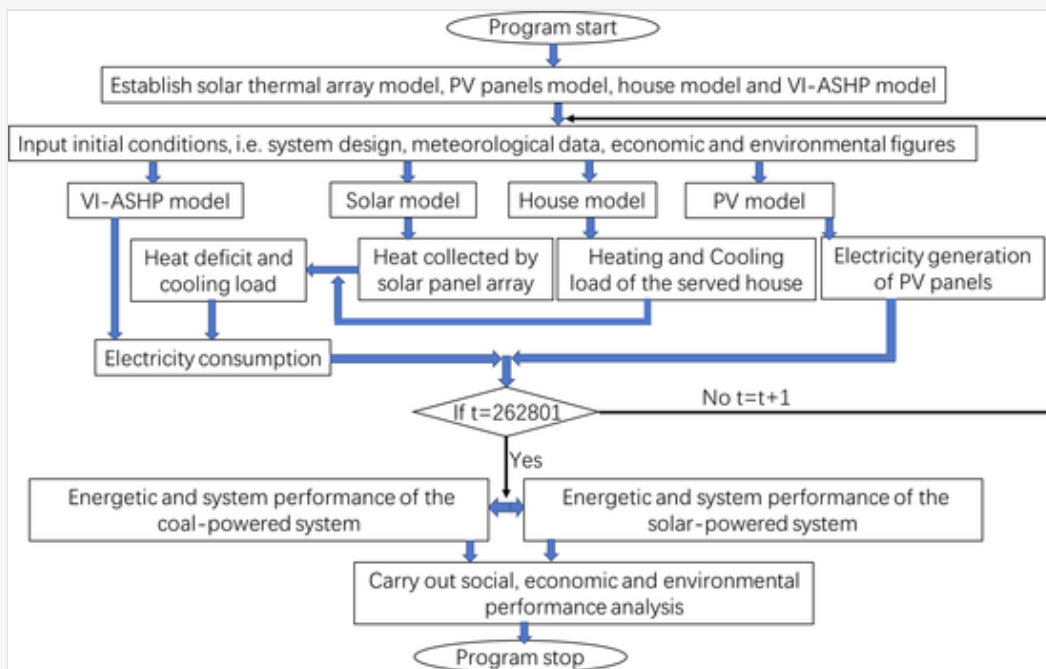
3 Mathematical models

The corresponding initial and boundary conditions, i.e. solar radiation, air temperature, wind speed and water temperature were extracted from the weather database by using Energy-Plus software (537720_CSXD) for Taiyuan[29]. During the operation of the model, it is assumed that the system works 24 h every day, and the heat pump operates at a condensation temperature of 50 °C for space heating in winter and an evaporation temperature of 10 °C for cooling in summer. The installation angles of solar PV and thermal panels are the same as the local altitude in the city. The economic figures, such as capital cost, renewable feed-in tariffs, system life span and air contaminant emission factors are also input into the program for calculation. The algorithm is presented in a flow diagram in Fig. 5, as explained below:

- (1) Input the design/operating parameters of the models for the solar thermal panel array, PV panels, house and VI-ASHP into program code.

- (2) Input the external boundary conditions from the weather data file, and divide the weather date into 262,800 parts throughout the year, thus giving a time step of 120 s. The calculation begins with the first weather data ($t = 1$).
- (3) Calculate the heating and cooling load, heat collected from the solar panel array, heat deficit, and electricity generated by the PV panels.
- (4) Calculate the electricity consumption of the system.
- (5) Move to the next step ($t = t + 120$) and repeat the calculation until $t = 262800$.
- (6) Carry out an energetic performance analysis of two systems.
- (7) Carry out an economic and environmental performance analysis of two systems.
- (8) Program stops.

Fig. 5



The calculation process of the model.

3.1 Heating and cooling load of the served house

The heating load of the served house in winter is mainly dependent on the difference between the room temperature (set at 16 °C) and the ambient temperature. It can be calculated based on the local weather data (Taiyuan city, Shanxi province).

The equation for the heating load can be given as:

$$Q_{h,l} = Q_{h,l.am} + Q_{h,l.wind}$$

(1)

In Eq. (1), the heating load of house envelops $Q_{h,l.am}$ can be expressed as:

$$Q_{h.l.am} = [(1 + \alpha_{h.l.e})S_{e,e} + (1 + \alpha_{h.l.w})S_{e,w} + (1 + \alpha_{h.l.s})S_{e,s} + (1 + \alpha_{h.l.n})S_{e,n}] \tau_{h.l} h_t (T_{r.hl} - T_a) \quad (2)$$

In order to take solar radiation as an impact factor, the orientation correction coefficients are integrated into the heat load calculation. In Eq.2, $\alpha_{h.l.e}$, $\alpha_{h.l.w}$, $\alpha_{h.l.s}$ and $\alpha_{h.l.n}$ are the coefficients of the house envelopes orientation correction facing east, west, south and north separately, and the values of which are -5% , -5% , -15% and 5% respectively [30]. $S_{e,e}$, $S_{e,w}$, $S_{e,s}$ and $S_{e,n}$ stand for the envelopes area facing corresponding direction, m^2 . In addition, the heating load of house cold air infiltration $Q_{h.l.wind}$ can be expressed as:

$$Q_{h.l.wind} = 0.28 C_{p,air} \rho_{air} L_{air} (T_{r.hl} - T_a) \quad (3)$$

In Eq.3, the cold air infiltration volume per hour L_{air} can be expressed as:

$$L_{air} = L_0 l_0 \quad (4)$$

In Eq.4, the cold air infiltration volume per hour per meter L_0 can be expressed as:

$$L_0 = \alpha_{air} \left(\frac{\rho_{air}}{2} v_0^2 \right)^b \quad (5)$$

In Eq.5, α_{air} is the coefficient of air permeability of outer doors and windows, $m^3/(m \cdot h \cdot Pa)$, the value of which can take 0.15 for residential building. v_0 is the local average wind velocity in the winter, m/s, the value of which can take 3.4 for Taiyuan city. b is the index of the air permeability of outer doors and windows, the value of which can take 0.67 for residential buildings [30].

The cooling load of the served house in summer is mainly determined by the difference between the room temperature (set at $24^\circ C$) and the ambient temperature. It can be calculated by:

$$Q_{c.l} = Q_{c.l.am} + Q_{c.l.solar} + Q_{c.l.people} \quad (6)$$

In Eq.6, the house envelopes cooling load $Q_{c.l.am}$ can be expressed as:

$$Q_{c.l.am} = \tau_{c.l} h_t S_e (T_{r.c.l} - T_a) \quad (7)$$

In Eq.6, the cooling load generated by solar radiation $Q_{c.l.solar}$ can be expressed as:

$$Q_{c.l.solar} = C_{clC}C_zD_{J.max}F_c$$

(8)

In Eq.8, C_{clC} is the solar radiation cooling load factor. The value of C_{clC} is determined by the orientation and the time and can be obtained from a local building design standard, *GB 50736-2012*. $D_{J.max}$ is the maximum index of the local solar radiation passing a glass in summer, which is 570 for Taiyuan city. The comprehensive shielding coefficient of the outer window C_z can be expressed as:

$$C_z = C_wC_nC_s$$

(9)

In Eq.9, C_w is the outer shielding device correction factor, C_n is the inner shielding device correction factor, C_s is the window glass correction factor. For the normal residential building with double-layer glass, C_w 0.95 is C_n is 0.9, and C_s is 1.

In Eq.6, the inner cooling load generated by body heat dissipation $Q_{c.l.people}$ can be expressed as:

$$Q_{c.l.people} = C_{people}\theta Q_{people}$$

(10)

In Eq.10, C_{people} is the number of people. θ is the clustering coefficient. Q_{people} is the maximum body heat dissipation generated by one person, W.

3.2 Collected solar energy by PV and solar thermal collectors

The collected energy from the solar system is divided into two parts, i.e. solar heat from the mini-channel panel array and electricity generated by the PV panels.

3.2.1 Collected solar thermal energy by mini-channel solar thermal panel array

The solar thermal energy output from the solar thermal panel array during the heating season can be expressed as:

$$Q_{st} = A_{st}I\eta_{ot}\tau_{st}$$

(11)

In the simulation, 8 thermal panels are connected in a multiple-throughout-flowing loop. The solar thermal efficiency of a single panel can be expressed as [9]:

$$\eta_{it} = 0.87 - 3.7 \frac{T_{in} - T_a}{I}$$

(12)

For each individual panel in a multiple-throughout-flowing configuration, the solar thermal efficiency is given by [9]:

$$\eta_1 = \left(\frac{Cp_w \dot{m} (t_1 - t_0)}{\frac{IA}{3}} + \frac{Cp_w \dot{m} (t_{16} - t_{15})}{\frac{IA}{3}} + \frac{Cp_w \dot{m} (t_{17} - t_{16})}{\frac{IA}{3}} \right) / 3 \quad (13)$$

$$\eta_2 = \left(\frac{Cp_w \dot{m} (t_2 - t_1)}{\frac{IA}{3}} + \frac{Cp_w \dot{m} (t_{15} - t_{14})}{\frac{IA}{3}} + \frac{Cp_w \dot{m} (t_{18} - t_{17})}{\frac{IA}{3}} \right) / 3 \quad (14)$$

$$\eta_3 = \left(\frac{Cp_w \dot{m} (t_3 - t_2)}{\frac{IA}{3}} + \frac{Cp_w \dot{m} (t_{14} - t_{13})}{\frac{IA}{3}} + \frac{Cp_w \dot{m} (t_{19} - t_{18})}{\frac{IA}{3}} \right) / 3 \quad (15)$$

$$\eta_4 = \left(\frac{Cp_w \dot{m} (t_4 - t_3)}{\frac{IA}{3}} + \frac{Cp_w \dot{m} (t_{13} - t_{12})}{\frac{IA}{3}} + \frac{Cp_w \dot{m} (t_{20} - t_{19})}{\frac{IA}{3}} \right) / 3 \quad (16)$$

$$\eta_5 = \left(\frac{Cp_w \dot{m} (t_5 - t_4)}{\frac{IA}{3}} + \frac{Cp_w \dot{m} (t_{12} - t_{11})}{\frac{IA}{3}} + \frac{Cp_w \dot{m} (t_{21} - t_{20})}{\frac{IA}{3}} \right) / 3 \quad (17)$$

$$\eta_6 = \left(\frac{Cp_w \dot{m} (t_6 - t_5)}{\frac{IA}{3}} + \frac{Cp_w \dot{m} (t_{11} - t_{10})}{\frac{IA}{3}} + \frac{Cp_w \dot{m} (t_{22} - t_{21})}{\frac{IA}{3}} \right) / 3 \quad (18)$$

$$\eta_7 = \left(\frac{Cp_w \dot{m} (t_7 - t_6)}{\frac{IA}{3}} + \frac{Cp_w \dot{m} (t_{10} - t_9)}{\frac{IA}{3}} + \frac{Cp_w \dot{m} (t_{23} - t_{22})}{\frac{IA}{3}} \right) / 3 \quad (19)$$

$$\eta_8 = \left(\frac{Cp_w \dot{m} (t_8 - t_7)}{\frac{IA}{3}} + \frac{Cp_w \dot{m} (t_9 - t_8)}{\frac{IA}{3}} + \frac{Cp_w \dot{m} (t_{24} - t_{23})}{\frac{IA}{3}} \right) / 3 \quad (20)$$

The overall solar thermal efficiency of the mini-channel solar thermal panel array can be expressed as:

$$\eta_{ot} = Cp_w \dot{m} (t_{24} - t_0) / (8IA) \quad (21)$$

3.2.2 Electricity generation by PV panels

The electricity generated by a PV panel can be expressed as[31]:

$$Q_{se} = NA_e I \eta_e \tau_{wy} \quad (22)$$

The photoelectric efficiency of the PV panel can be expressed as:

$$\eta_e = \eta_{rc} [1 - \beta_{PV} (T_c - T_{rc})] \quad (23)$$

The temperature of the PV cell can be expressed as:

$$T_c = T_a + \frac{(NOTC - 20)}{0.8} I \quad (24)$$

3.3 Energy consumption of the systems

3.3.0.1 Electricity consumption of the VI-ASHP

The electricity consumed by the VI-ASHP for winter heating can be expressed as[32]:

$$Q_{ec.wh} = \frac{Q_{hd}}{COP} \quad (25)$$

Q_{hd} is the heat deficit of the system, which can be expressed as:

$$Q_{hd} = Q_{h,l} - Q_{st} \quad (26)$$

The electricity consumed by the VI-ASHP for summer cooling can be expressed as[32]:

$$Q_{ec.sc} = \frac{Q_{cl}}{EER} \quad (27)$$

Cooperating with the mini-channel solar thermal panel array, a VI-ASHP is applied to provide heating in winter and cooling in summer. The coefficient of performance for winter heating (COP) and energy efficiency ratio for

summer cooling (EER) are modelled based on the performance of a commercialised VI-ASHP by Emerson Electric Co. [33]. COP can be expressed as:

$$COP = \frac{Q_{hp}}{W_{ec}} \quad (28)$$

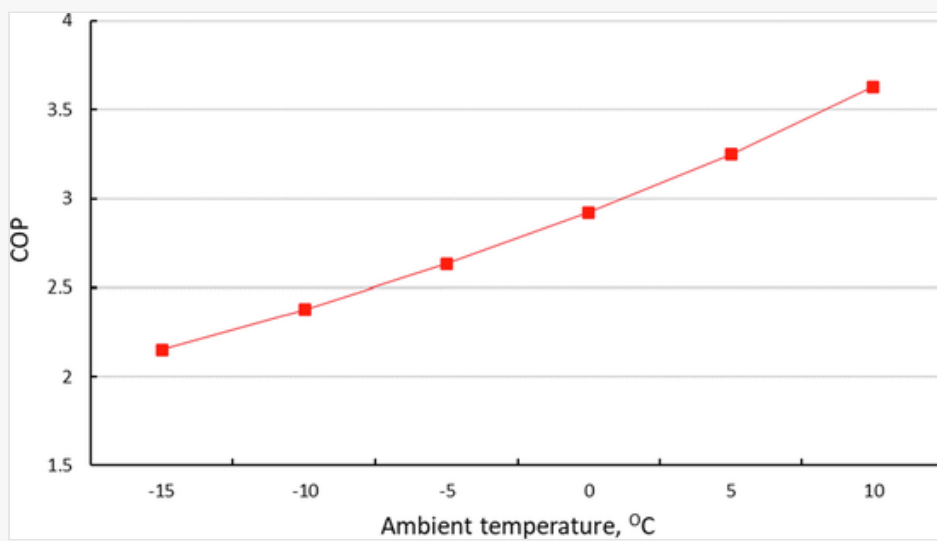
EER can be expressed as [34]:

$$EER = \frac{Q_{cp}}{W_{ec}} \quad (29)$$

In winter the VI-ASHP operates at a condensation temperature of 50 °C for space heating. Within the evaporator, the temperature difference between ambient air and exhaust air is 5 °C. Similarly, the temperature difference between the exhaust air and the evaporation temperature is also 5 °C, leading to a temperature difference between ambient temperature and evaporation temperature of refrigerant of 10 °C. The performance of the VI-ASHP for heating is shown in Fig. 6. According to the performance curve, the relationship between ambient temperature and COP can be expressed as:

$$COP = 0.000764575 * T_{am}^2 + 0.062569118 * T_{am} + 2.922993 \quad (30)$$

Fig. 6



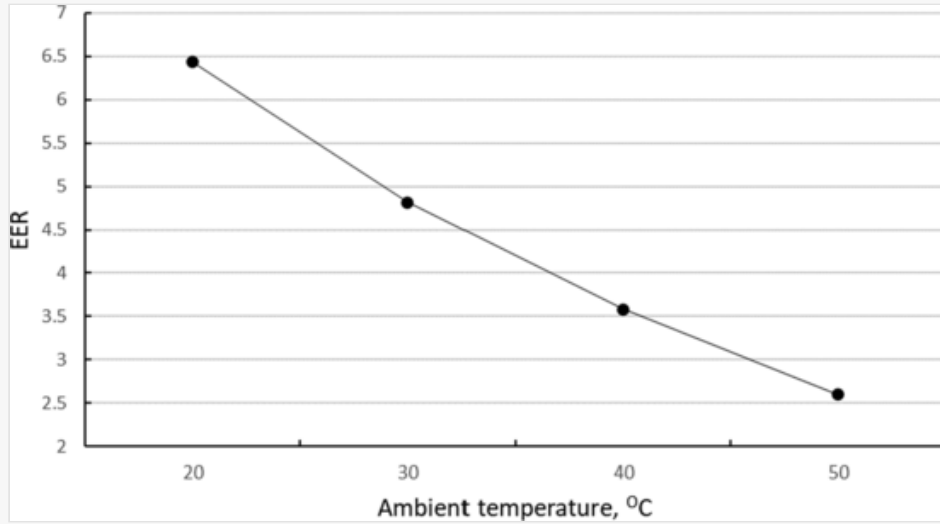
The COP of the VI-ASHP in heating.

In summer, the VI-ASHP operates in cooling mode, in which the evaporation temperature is set to 10 °C for cooling. Similarly, with the heating mode, the temperature difference between the ambient air and condensation temperature of the refrigerant is 10 °C. The performance of the VI-ASHP for cooling is shown in Fig. 7.

According to the performance curve, the relationship between ambient temperature and EER can be expressed as:

$$EER = 0.001591963 * T_{am}^2 - 0.238768127 * T_{am} + 10.56483 \quad (31)$$

Fig. 7



The EER of the VI-ASHP in cooling.

3.3.0.2 Electricity consumption of the water pump

The electricity consumed by the water pump of the system can be expressed as:

$$Q_{ec.wp} = P_{wp} \hat{A} \cdot \tau_{wp} \quad (32)$$

3.3.0.3 Coal consumption of the coal-based system

The coal consumed by a coal-powered system can be given as:

$$Q_d = q_c m_{c.c} \eta_c \quad (33)$$

Where q_c is the calorific value generated by anthracite coal, which is 8 kWh/kg [35]; $m_{c.c}$ is the consumed anthracite coal by a coal-based heating system, kg; η_c is the heating efficiency, which is 75% in the simulation [36].

3.4 Economic analysis of the systems

The initial capital cost of the novel solar-assisted VI-ASHP space heating system includes the individual cost of all the system components. A mark up of 20% is adopted to allow for commercial profits. The basic equipment cost is mainly divided into five parts: the solar thermal panel array; PV panels; heat storage and exchange unit; VI-ASHP and all other miscellaneous costs, which include additional equipment such as pipes and pipe fittings, water pump, grid inverter and installation cost. Consequently, the initial capital cost can be expressed as:

$$C_{c,sp} = (C_{PT} + C_{PV} + C_{HSEU} + C_{HP} + C_{ADD})\hat{A} \cdot (1 + 20\%) \quad (34)$$

The other cost C_{ADD} is assumed to be 10% of the equipment cost, and is expressed as[37]:

$$C_{ADD} = (C_{PT} + C_{PV} + C_{HSEU} + C_{HP})\hat{A} \cdot 10\% \quad (35)$$

The equivalent payback period (PP) of this novel solar-assisted VI-ASHP system to replace a conventional coal-based system can be expressed as[37]:

$$PP_{sp} = \frac{\text{Capital Cost} - \text{Incentives}}{\text{Annual (Operational \& maintenance) Cost Saving}}$$

$$PP_{sp-c} = \frac{C_{c,sp} - C_{c,c} - C_{RE}}{(C_{o,c} + C_{m,c}) - (C_{o,sp} + C_{m,sp})} \quad (36)$$

Where $C_{o,sp}$ and $C_{m,sp}$ are operational and maintenance costs of the novel system.

To support the installation of a renewable energy system it may be possible to receive grants through the government's renewable policy. For example, the Renewable Heat Incentive (RHI) scheme is intended to encourage the uptake of renewable heating technologies within households, communities and businesses through the provision of financial incentives. Whilst there is currently no financial incentive for solar thermal energy, the current feed-in tariff price for photovoltaic electricity is '¥0.75/kWh' for Shanxi[38]. As a result, the ultimate operational cost of such a system equals the basic operational cost including the operational cost by the VI-ASHP and water pumps minus the total earning of the generated electricity, which can be expressed by

$$C_{o,sp} = C_{o,hp} + C_{o,wp} - C_{te} \quad (37)$$

The maintenance cost of the three systems is normally estimated at 2% of the initial system cost[39]. As a solar-based system is usually considered to have a lifespan of 25 years[40], the life-cycle net cost saving, CS_{sp} , of this system in energy bills can be determined by

$$CS_{sp} = (Lifetime - paybacktime) \times Annual (Operational \& maintenance) Cost Saving$$

$$CS_{sp-c} = (25 - PP_{sp-c}) [(C_{o,c} + C_{m,c}) - (C_{o,sp} + C_{m,sp})] \quad (38)$$

3.5 Contaminants analysis

Four kinds of air contaminations, CO₂, harmful dust, SO₂, and NO_x, are taken into consideration in this paper and the quantity can be expressed as:

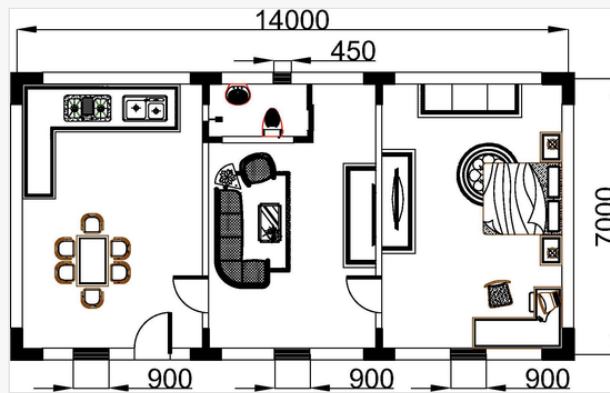
$$m_{p,c} = m_{pu,c} m_{c,c} \quad (39)$$

Where $m_{p,c}$ is the mass of air contaminations generated by the coal-based heating system, kg; and $m_{pu,c}$ is the mass of air contaminations generated by per unit anthracite coal separately, kg/kg.

4 Case study model

In this section, a rural house located in Taiyuan City, Shanxi Province in northern China (37.52°N, 111.15°E) is selected as a case study. The system provides space heating, cooling, and domestic hot water flexibly. The served house has an area of 100 m², a length of 14 m, a width of 7 m and a height of 4 m. The front façade of the house faces south. The schematic of the served house is shown in Fig. 8, and the heat transfer coefficients of the building envelopes are listed in Table 2. The thermal properties of the building components are the same as the actual parameters for a common rural house, thus providing an accurate reflection of the heat load for a rural house.

Fig. 8



The floor plan and corresponding dimensions of the served house.

Table 2

The table layout displayed in this section is not how it will appear in the final version. The representation below is



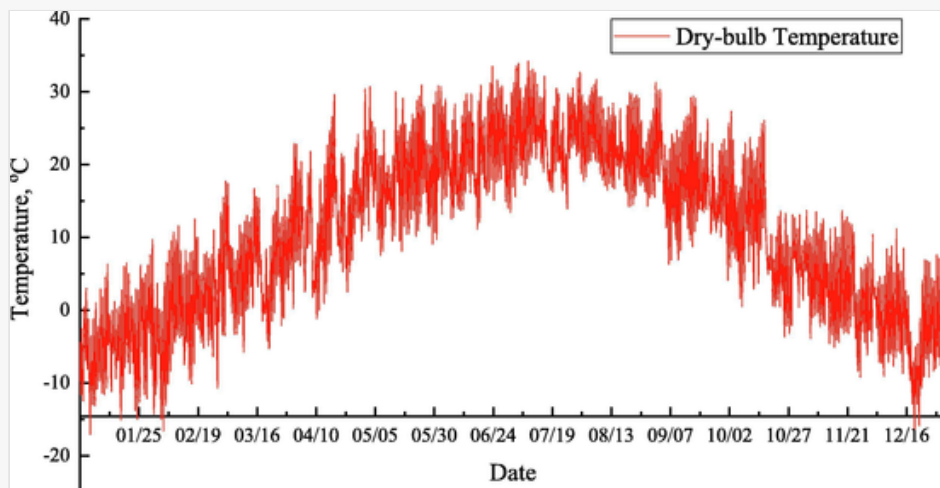
solely purposed for providing corrections to the table. To preview the actual presentation of the table, please view the Proof.

The heat transfer coefficients of the building envelope.

Part	Structure	K [W/(m ² ·°C)]
Wall	370 mm brick wall Plastering + 50 mm extruded polystyrene board	0.47
External doors	Pinewood door	2.9
Window	3 mm common glass aluminium alloy window frame (two layers)	1.54
Roof	Cement mortar + Insulation layer + Waterproof layer + Tile.	0.37

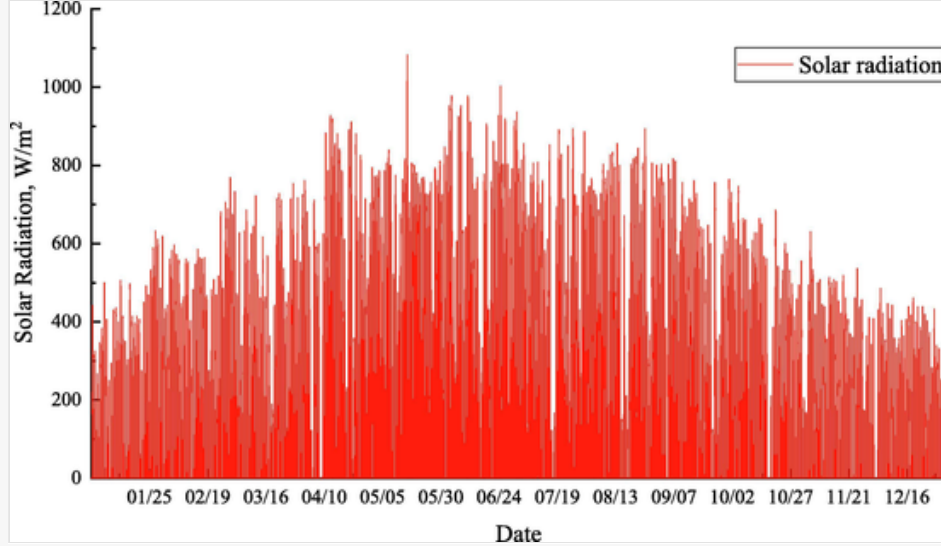
The hourly dry-bulb ambient temperature and the solar radiation variation for a whole year in Taiyuan city are shown in Fig. 9 and Fig. 10 separately. The ambient dry-bulb temperature varies from $-15\text{ }^{\circ}\text{C}$ to $35\text{ }^{\circ}\text{C}$. The highest ambient dry-bulb temperature reaches $35\text{ }^{\circ}\text{C}$ on the initial days of July, and the lowest ambient temperature reaches $-15\text{ }^{\circ}\text{C}$ during January.

Fig. 9



The hourly ambient dry-bulb temperature variation along a year.

Fig. 10



The hourly solar radiation variation along a year.

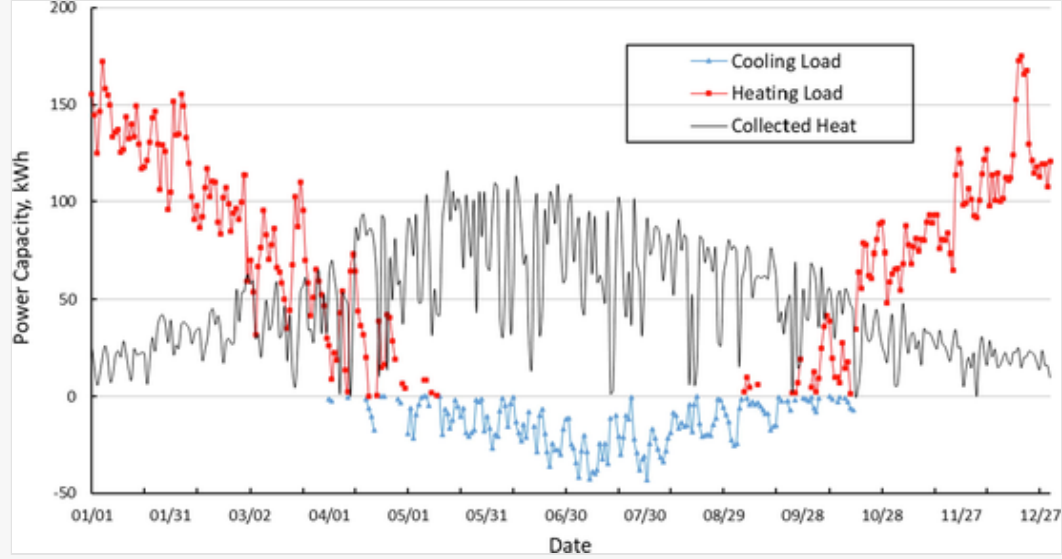
The hourly solar radiation variation is similar to the trend of ambient temperature which is shown in Fig. 10. During the summer months, from May to August, the highest solar radiation can reach 900 W/m^2 to 1000 W/m^2 . And during the winter months, from November to December, the lowest solar radiation falls to 400 W/m^2 to 500 W/m^2 .

5 Results and discussion

5.1 Thermal performance

According to the local weather conditions, the daily collected solar heat, daily heating load during winter and daily cooling load during summer can be simulated as shown in Fig. 11. During the heating season in winter, the heat load often surpasses the collected heat due to the low solar radiation and ambient temperature. More panels can be employed to increase the solar heat gain; however, the roof area and cost limit this option. During some periods from the 1st of April to the 15th of May and from the 1st of September to the 10th of October, both cooling and heating are required in a single day. Nonetheless, owing to the flexibility of the proposed system, it can perfectly fit the polytropic and complicated thermal environment, and maintain the room temperature at a relatively stable range, i.e. $16 \text{ }^\circ\text{C}$ to $24 \text{ }^\circ\text{C}$.

Fig. 11



Daily variations of the solar energy collection, heating and cooling load along a year.

Table 3 shows the monthly collected heat, heating load and cooling load summarized from Fig. 11. The annual space heating load and the collected heat of the system are 17538kWh and 17770kWh separately. From January to April, and October to December, the heat load is higher than the collected heat, the highest monthly heat deficit peaks at 3465.3kWh in January and the total heat deficit is 12010.6kWh for the winter months. From May to September, the collected heat is higher than the heat load and most solar heat can be used to generate domestic hot water, which is a good advantage of the system. Due to the spare heat from May to September, the system can provide a total of 274.5 tons of domestic hot water, which can save 12262.6kWh of energy. The annual cooling load of the house is 2311kWh.

Table 3

i The table layout displayed in this section is not how it will appear in the final version. The representation below is solely for providing corrections to the table. To preview the actual presentation of the table, please view the Proof.

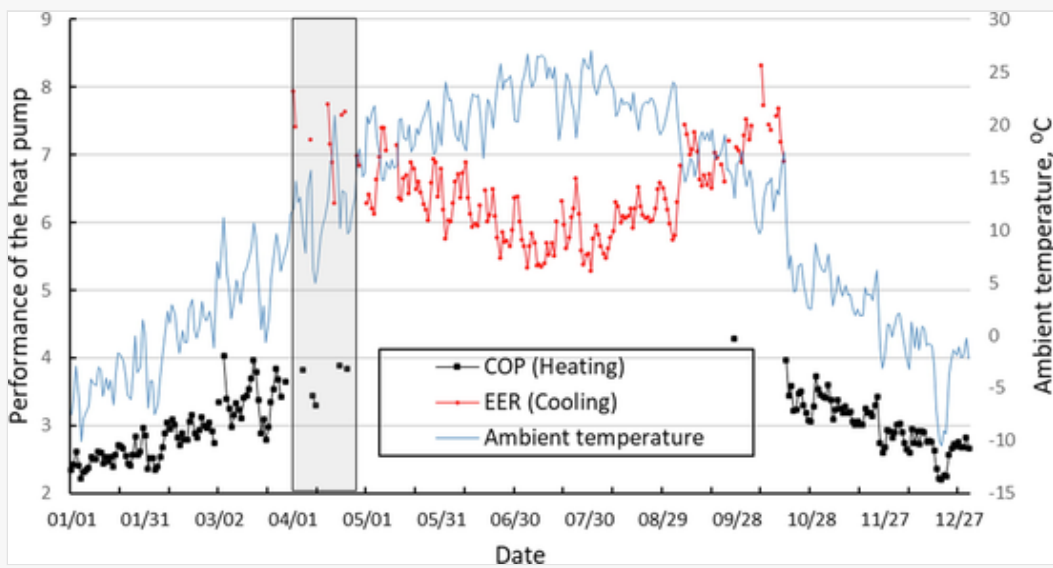
Monthly heating and cooling load and heat deficit.

Month	Jan	Feb	Mar	Apr	May	Jun
Cooling Load (kWh)	0	0	0	43.89	263.6	495.57
Heating Load (kWh)	4161.98	3055.84	2028.57	736.25	19.03	0
Heat Deficit (kWh)	3465.31	2098.64	785.32	198.63	0	0
Month	Jul	Aug	Sep	Oct	Nov	Dec
Cooling Load (kWh)	798.45	480.54	190.37	38.16	0	0

Heating Load (kWh)	0	0	53.56	1224.82	2525.56	3732.83
Heat Deficit (kWh)	0	0	0	552.12	1721.72	3142.04

Given the ambient temperature, the daily average COP in winter and EER in summer of VI-ASHP are shown in Fig. 12. The results show that the EER of the VI-ASHP is higher than the COP, indicating that the electricity consumption for winter heating will be higher than that for summer cooling at the same load. Considering the heating load is significantly higher than the cooling load, the device selection of VI-ASHP in temperate continental monsoon climate areas, such as Taiyuan city, should put heating performance a priority. Moreover, the shaded area in Fig.21 shows that the VI-ASHP needs to supply heating and cooling during a single day to keep a high level of indoor thermal comfort.

Fig. 12



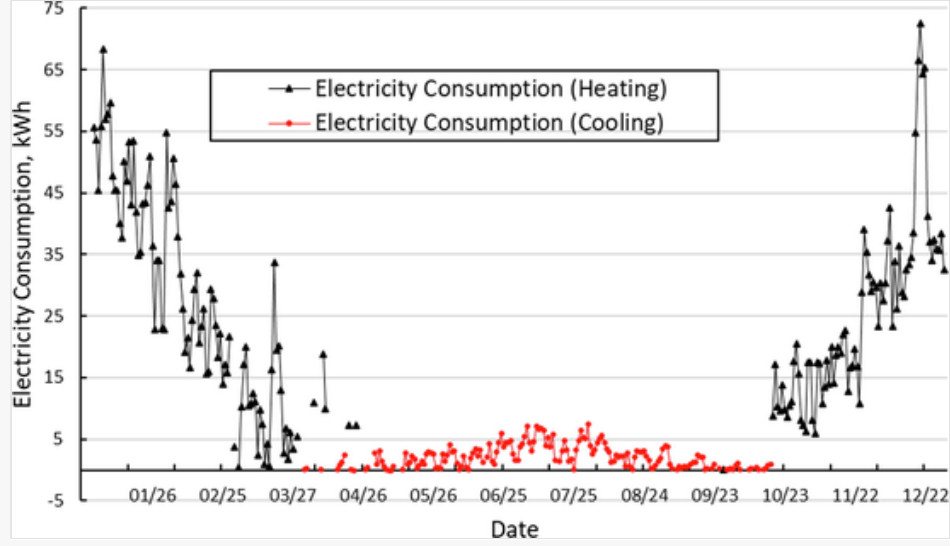
The daily COP and EER variations of the VI-ASHP over a whole year.

5.2 Electrical performance

5.2.1 Electricity consumption of the system

The heat deficit can be calculated by the difference between the heating load and heat collection. In addition, as shown in Fig. 13, the daily electricity consumption of the system can be obtained based on heat deficit in winter, cooling load in summer, COP and EER of the VI-ASHP. Obviously, the electricity consumption of heating during the winter is much higher than that of cooling during the summer. The daily electricity consumption for heating peaks at 74kWh in December, while the highest electricity consumption for cooling is just 8kWh in July.

Fig. 13



The daily electricity consumption for the VI-ASHP over a year.

As shown in [Table 4](#), the electricity consumed for winter heating is a totally 4394.6kWh and the electricity consumed for summer cooling is a totally 355.2kWh. This gives an annual total electricity consumption by the VI-ASHP of 4749.8kWh. The power of a water pump is 400 W. According to the operation time of the system, the pump power can be determined, as shown in [Table 5](#). The total electricity consumption for the pump is 1290.4kWh. According to the above analysis, the total annual electricity consumption of the system is 6040.2kWh.

Table 4

i The table layout displayed in this section is not how it will appear in the final version. The representation below is solely purposed for providing corrections to the table. To preview the actual presentation of the table, please view the Proof.

Monthly electricity consumption of the heat pump.

Month	Jan	Feb	Mar	Apr	May	Jun
Electricity Consumption (Heating) (kWh)	1385.9	768.81	251.14	54.25	0	0
Electricity Consumption (Cooling) (kWh)	0	0	0	3.84	24.09	48.11
Month	Jul	Aug	Sep	Oct	Nov	Dec
Electricity Consumption (Heating) (kWh)	0	0	0.17	168.79	571.19	1194.32
Electricity Consumption (Cooling) (kWh)	81.72	46.92	17.50	3.15	0	0

Table 5

i The table layout displayed in this section is not how it will appear in the final version. The representation below is solely for providing corrections to the table. To preview the actual presentation of the table, please view the Proof.

Monthly operation time of the water pump.

Month	Jan	Feb	Mar	Apr	May	Jun
Monthly Water Pump Operation Time (h)	219	229	269	285	352	317
Month	Jul	Aug	Sep	Oct	Nov	Dec
Monthly Water Pump Operation Time (h)	311	302	267	246	219	210

5.2.2 Electricity generation of the system

There are four photovoltaic panels, and each has an aperture area of 2 m². The electricity generation per square meter every month is shown in Table 6, which is 216.2 kWh/m² annually. Hence, the total photovoltaic electricity production is 1729.6kWh. The feed-in tariff in Shanxi is 0.75RMB/kWh, which means that the served house can earn a total of 1297.2RMB per year by transferring the generated electricity into the power grid.

Table 6

i The table layout displayed in this section is not how it will appear in the final version. The representation below is solely for providing corrections to the table. To preview the actual presentation of the table, please view the Proof.

Electricity generated monthly per square meter of PV panel.

month	1	2	3	4	5	6	7	8	9	10	11	12
Solar irradiation (W/m ²)	254	333	344	414	488	446	401	396	336	322	270	229
Ambient temperature (°C)	-2.3	2.0	8.3	14.7	21.3	24	26	24.2	20.1	13.2	5.8	0
Total working time (hours)	283	256	310	340	372	360	372	372	360	316	270	279
Average electrical efficiency	19.4%	18.9%	18.3%	17.6%	16.8%	16.7%	16.7%	16.7%	17.4%	18%	18.7%	19.3%
Electricity generated	12.3	14.1	17.1	21.7	26.8	23.5	21.8	21.7	18.4	16.0	12.0	10.8

(kWh)

According to the monthly electricity price as displayed in Table 7, the annually earned money from PV panels in the system can buy 1633kWh of electricity from the grid. The monthly electricity consumption and the corresponding cost of the whole system are shown in Table 8. The electricity cost in January and December is remarkably higher than that in other months, since the low ambient temperature is accompanied by a high heat load for the building. The total annual electricity cost for the system is 3886RMB. Taking into account the earned 1297.2RMB, the annual operational cost of the system is 2589RMB for space heating, cooling and hot water supply. Overall, the photovoltaic profit provides 27% of the total operation cost, thereby making the system more economic and considerably decreasing fossil fuel consumption.

Table 7

i The table layout displayed in this section is not how it will appear in the final version. The representation below is solely purposed for providing corrections to the table. To preview the actual presentation of the table, please view the Proof.

The electricity utility price.

Utility price (RMB/kWh) [41]	$X \leq 170$ kWh	$171 < X \leq 260$ kWh	$X > 260$ kWh
	0.477	0.527	0.777

Table 8

i The table layout displayed in this section is not how it will appear in the final version. The representation below is solely purposed for providing corrections to the table. To preview the actual presentation of the table, please view the Proof.

Monthly system electricity consumption and cost.

Month	Jan	Feb	Mar	Apr	May	Jun
Electricity Consumption (kWh)	1473.51	860.41	358.74	174.17	178.30	202.64
Electricity Cost (RMB)	1071.41	595.04	205.24	76.89	78.65	98.29
Month	Jul	Aug	Sep	Oct	Nov	Dec
Electricity Consumption (kWh)	254.33	194.83	134.23	271.95	658.79	1278.33
Electricity Cost (RMB)	125.53	80.00	59.29	137.81	438.38	919.76

5.3 Energy proportions of the system

The energy proportions of the system in terms of all energy sources are shown in [Table 9](#), based on the total annual solar thermal energy output and electrical consumption of the system. It is shown that to support the space heating of the simulated house, the energy volumes provided by solar thermal energy, photovoltaic energy and electricity from the power grid are 74.6%, 6.9%, and 18.5% respectively. Hence, the energy supply proportion is about 81.5% from solar energy, and thus the primary energy source of the system mainly is solar energy.

Table 9

i The table layout displayed in this section is not how it will appear in the final version. The representation below is solely purposed for providing corrections to the table. To preview the actual presentation of the table, please view the Proof.

Annual energy usage breakdowns of the system.

Energy Breakdown	Value (kWh)	Radio (%)
Solar Thermal Energy	17,770	74.6
Photovoltaic Electricity	1633	6.9
Electricity	4407	18.5

5.4 Economic performance

5.4.1 The capital cost of the system

Because the case study is set under the weather conditions in northern China, the economic analysis in this paper is based on the Chinese market. The initial capital cost of the proposed system is 30290RMB, and a cost breakdown is shown in [Table 10](#). Furthermore, the cost details of the components are presented in [Fig. 14](#). The VI-ASHP is the most expensive component of the system, accounting for nearly 34% of the total cost. Compared with the solar assisted VI-ASHP system, the coal-based a heating system has a lower initial capital cost of 10400RMB.

Table 10

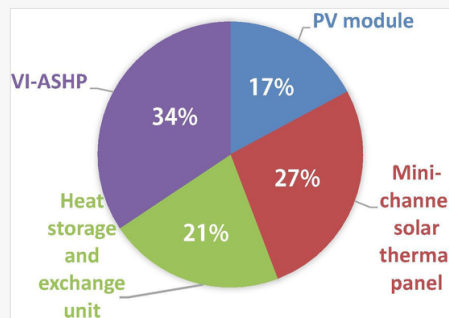
i The table layout displayed in this section is not how it will appear in the final version. The representation below is solely purposed for providing corrections to the table. To preview the actual presentation of the table, please view the Proof.

Initial capital cost of the systems.

<i>Solar assisted VI-ASHP system</i>				
No.	Component	Quantity/Size	Unit Price (RMB)	Cost (RMB)
1	PV panels	4	1000	4000
2	Solar thermal panels	8	787.5	6300

3	Heat storage and exchange unit	1	5000	5000
4	VI-ASHP	1	8000	8000
Additional cost				10%
Additional profit				20%
Initial capital cost (RMB)				30,290
<i>Coal-driven system</i>				
No.	Component	Quantity/Size	Unit Price (RMB)	Cost (RMB)
1	Coal boiler	1	8000	8000
Additional cost				10%
Additional profit				20%
Initial capital cost (RMB)				10,400

Fig. 14



Cost details of the different system components.

5.4.2 Operational cost, life-cycle and cost payback period compared to the conventional heating system

As discussed above the heat deficit during the space heating season is 12010.6kWh and the collected solar thermal energy is 17770kWh. This means that the system needs a total heat of 29780.6kWh annually to provide space heating and domestic hot water.

The annual maintenance cost of a solar heating system is normally estimated at 2% of the initial system cost, and the annual operating cost of these systems can be estimated as shown in [Table 11](#). Compared with the coal-driven system, this novel system has a cost payback period of 6.52 years and a life-cycle net cost saving of nearly 56328.4RMB in Shanxi. The results show the superior economic performance of the novel solar-powered system.

Table 11

i The table layout displayed in this section is not how it will appear in the final version. The representation below is solely purposed for providing corrections to the table. To preview the actual presentation of the table, please view

Annual operating costs, cost payback period and Life-cycle cost saving.

<i>Solar assisted VI-ASHP system operational performance</i>	
The heat produced by solar thermal panel array (kWh/yr.)	17,770
The energy required from VI-ASHP (kWh/yr.)	11,687
Total electricity output from the PV module (kWh/yr.)	1729.6
Electricity consumed by VI-ASHP (kWh/yr.)	4750
Electricity consumed by the water pump (kWh/yr.)	1290.4
Operational cost (RMB/yr.)	2589
Maintenance fee (RMB/yr.)	717.6
<i>Coal-based system (efficiency 75%)</i>	
Coal price (Anthracite Coal) (¥/kWh) ^[42]	0.152
Capital cost (RMB)	10,400
Required coal energy (kWh/yr.)	39707.4
Operational cost (RMB/yr.)	6035.5
Maintenance fee (RMB /yr.)	208
Payback period of the solar-powered space heating system (yr.)	6.52
Life-cycle cost-saving (RMB)	56328.4
Per m ² life-cycle cost-saving (RMB/m ²)	563.3


5.5 Environmental performance

5.5.1 Annual fossil fuel saving and carbon emission reduction

Coal is the most common energy source used for conventional heating systems in northern China, with a typical efficiency of 75% for a domestic heating system. The heat generated by burning 1 kg of anthracite coal is 8kWh, which means the annual fossil fuel requirement for a standard Chinese northern rural house will be 4963.4 kg. This amount of coal can be avoided by using the proposed solar energy system.

As a result of the combustion of fossil fuel, harmful dust and other pollutants will be diffused into the air and cause severe pollution and global warming. The air contaminants generated from the combustion of 1 kg of anthracite coal are shown in [Table 12](#), and the annual contaminants for a standard Chinese northern rural house are shown in [Table 13](#).

Table 12

 The table layout displayed in this section is not how it will appear in the final version. The representation below is

solely purposed for providing corrections to the table. To preview the actual presentation of the table, please view the Proof.

The contaminants generated by per unit anthracite coal [43]

Per unit fossil fuel	Harmful dust	CO ₂	SO ₂	NO _x
Anthracite Coal /kg	0.0068 kg	2.57 kg	0.02 kg	0.004 kg

Table 13

i The table layout displayed in this section is not how it will appear in the final version. The representation below is solely purposed for providing corrections to the table. To preview the actual presentation of the table, please view the Proof.

The annual contaminants generated by coal-driven system.

Contaminants	Coal-powered(kg)
Harmful dust	33.7
CO ₂	12110.7
SO ₂	372.2
NO _x	186.1

The reduction of contaminants by the solar assisted VI-ASHP system is highlighted in Table 14, on the assumption that 100 sets of the systems (e.g., to meet the demand of a village) are used. The reductions of fossil fuel consumption and pollutants are significant. In one year, the solar-based energy system could save 496.3tons of coal. During the 25-year life span of the systems, the total carbon emission savings could reach 30276.7tons compared with the coal-based system. Furthermore, the system diminishes the emission of a lot of other harmful substances, i.e. dust, SO₂ and NO_x, and therefore is a desirable approach to the environment sustainability.

Table 14

i The table layout displayed in this section is not how it will appear in the final version. The representation below is solely purposed for providing corrections to the table. To preview the actual presentation of the table, please view the Proof.

fossil fuel saving and air pollutant reduction.

	Contaminants	2018	25 years total
Solar-based system compared with coal-based system	Mass (tons)	496.3	12407.5
	Harmful dust (tons)	3.4	84.4

CO ₂ (tons)	1211	30276.7
SO ₂ (tons)	37.2	930.6
NO _x (tons)	18.6	465.3

6 System demonstration and experimental validation

6.1 Mini-channel multiple-throughout-flowing solar array

A demonstration project of the mini-channel solar-assisted air source heat pump system, which is similar to the proposed system, has been installed in a rural village of Shanxi province, as shown in Fig. 15[44]. The technical parameters of the demonstrative system are shown in Table 15. The mini-channel solar thermal panels are connected in a multiple-throughout-flowing loop as mentioned in the simulation of the proposed system. In addition, there are two solar panel arrays containing 10 and 8 panels respectively. The systems can greatly increase the thermal comfort in rural houses and significantly decrease fossil fuel consumption and environmental contaminations.

Fig. 15



The demonstration of the solar energy systems installed at the demonstration site.

Table 15

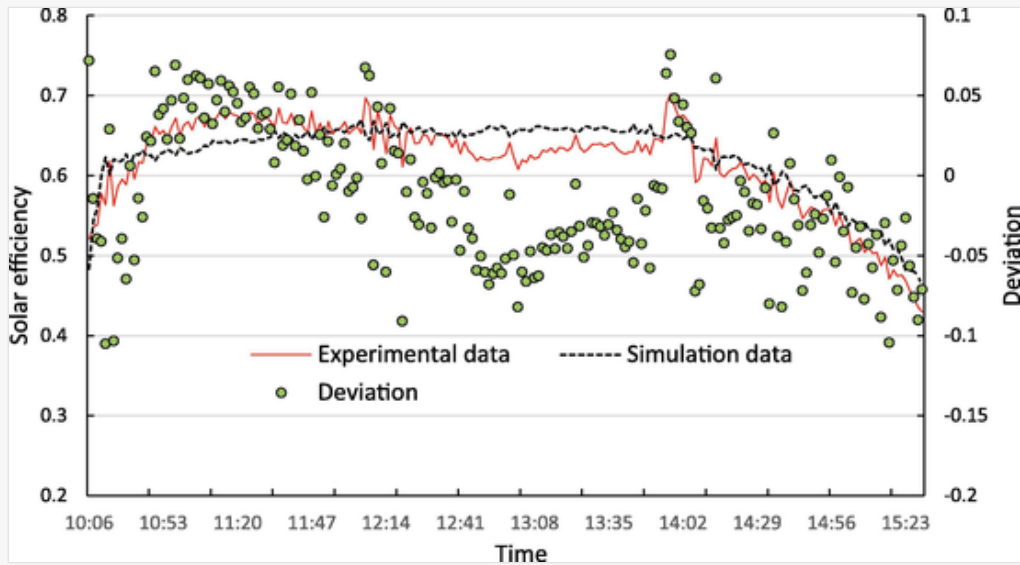
i The table layout displayed in this section is not how it will appear in the final version. The representation below is solely purposed for providing corrections to the table. To preview the actual presentation of the table, please view the Proof.

Technical parameters of the system.

Component	Size	Number
Mini-channel solar thermal panels	1 m*2 m	18
Photovoltaic panels	1 m*2 m	4
Heat exchange and storage water tank	1.5 t	1
Air source heat pump (Nominal heat supply capacity: 12 kW)	1.2 m*0.5 m*1 m	1

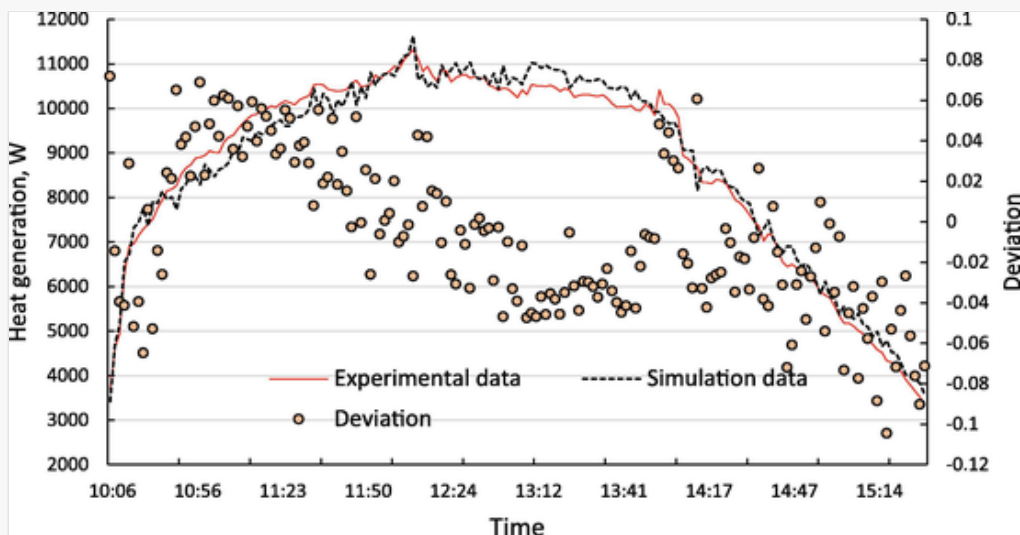
The experimental data from this demonstrative project can verify the model for the simulation of the performance of the mini-channel solar panel array. The experimental and simulated results are compared in Fig. 16 and Fig. 17. The tests were conducted on the 24th of Dec 2016. The experimental and simulative results for solar thermal efficiency and heat generation are in good agreement, within 10% deviation, which validates the proposed model.

Fig. 16



The experimental and simulative solar efficiency of the solar thermal panel arrays.

Fig. 17



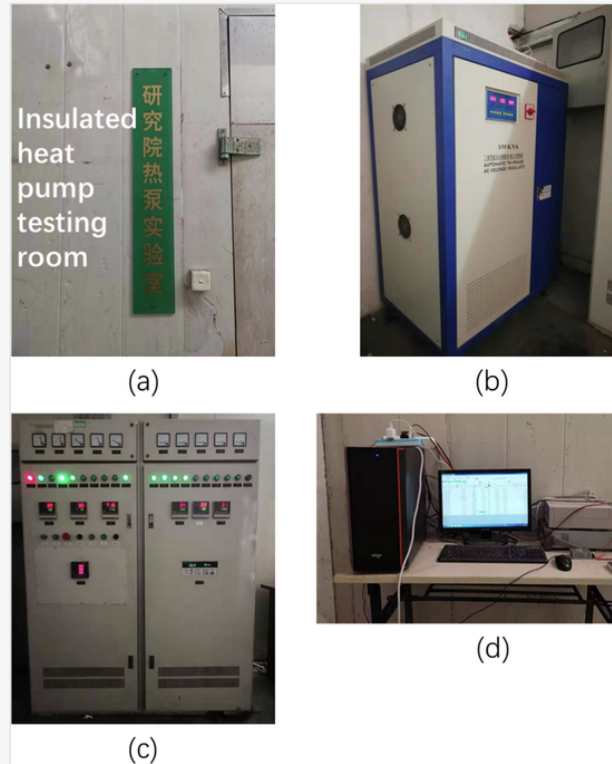
The experimental and simulative heat generation of the solar thermal panel arrays.

6.2 VI-ASHP_{xxx}

To validate the mathematical model of the VI-ASHP, indoor experimental tests were conducted in a heat pump test room at Five-star Solar Energy Co. Ltd. The test room contains four key components: (1) an insulated room where the tested heat pump can be placed, as shown in Fig. 18(a); (2) an electrical power source for the whole

system, as shown in Fig. 18(b) to provide power to the heat pump, testing room cooling devices, water pumps, control device and data collecting device; (3) an environment control device as shown in Fig. 18(c) which can collect timely temperature and humidity data from the testing room and maintain the parameters at the desired level, and the error of the controlled temperature is about within ± 1.5 °C; and (4) a data-collecting device as shown in Fig. 18(d) which can collect experimental data from the pre-positioned sensors, and thus calculate the heat pump performance, i.e. heat generation, electricity consumption, COP, and EER.

Fig. 18



The experimental equipment of VI-ASHP (a) insulated heat pump testing room; (b) electricity power source; (c) environment control devices; (d) data collection devices.

The experimental set up for our VI-ASHP is shown in Fig. 19, whilst the technical parameters are shown in Table 16.

Fig. 19



The experiment of VI-ASHP.

Table 16

i The table layout displayed in this section is not how it will appear in the final version. The representation below is solely purposed for providing corrections to the table. To preview the actual presentation of the table, please view the Proof.

Technical parameters of the VI-ASHP.

Model	DKRS-20	Refrigerant	R410A
Nominal heating power (kW)	39	Nominal power input (Heating, kW)	16.18
Nominal cooling power (kW)	48	Nominal power input (Cooling, kW)	17.9
Max current (A)	50	Max power (kW)	27
Working temperature (°C)	−20–43	Rated voltage (V)	380

The performance of the demonstrative VI-ASHP system can be simulated by using the model developed in this paper. Comparing the experimental data of the demonstrative VI-ASHP system under $-11.5\text{ }^{\circ}\text{C}$, the simulation results are in close agreement with the experimental results, with the deviation between results of less than 6.2% as shown in Table 17. The results fully illustrate the validity of our proposed model. VI-ASHP demonstration systems have also been built in northern China, which are shown in Fig. 20.

Table 17

i The table layout displayed in this section is not how it will appear in the final version. The representation below is solely purposed for providing corrections to the table. To preview the actual presentation of the table, please view the Proof.

Comparison between experimental and simulative performance of VI-ASHP.

Ambient temperature ($^{\circ}\text{C}$)	-11.46	-11.48	-11.47	-11.46	-11.45	-11.46	-11.45
Power input (kW)	13.26	13.24	13.20	13.19	13.17	13.19	13.16
Heat generation (kW)	28.24	28.46	28.51	28.356	28.32	28.22	28.29
COP (Experiment)	2.13	2.15	2.16	2.15	2.15	2.14	2.15
COP (Simulation)	2.17	2.17	2.17	2.17	2.17	2.17	2.17
Deviation (%)	5.1	5.7	6.2	5.7	5.8	5.2	5.8

Fig. 20



The demonstration project of VI-ASHP installed.

7 Conclusion

This paper proposed a dedicated economic and environmental performance study of a novel low carbon solar-assisted vapour injection air source heat pump (VI-ASHP) system for space heating, cooling and domestic hot water system in cold regions. The simulation is conducted based on the weather conditions of Taiyuan, Shanxi, northern China, as this city uses coal as the main energy source to supply space heating. Consequently, the city suffers from severe air pollution and desperately needs to use renewable energy to improve the life quality and environment for local residents. The simulation results involve the prediction of fossil fuel energy savings, cost payback period on investment and life cycle carbon emission reduction of the novel system, compared to conventional coal-based heating systems.

The mini-channel solar thermal panel array of 36 m² and VI-ASHP of 40 kW have been successfully demonstrated. Experiments have been conducted and the results validate the mathematical models established in this paper. According to the analysis, the relative deviation between the established models and the experimental data is within 10%, thus giving high accuracy.

The energy performances of the proposed solar-assisted VI-ASHP system and the served house are simulated and the results indicate that the heating load and cooling load for the 100 m² served house are 17538kWh and 2311kWh respectively. The heat generated from the solar thermal panel array is 17770kWh. To overcome this heat deficit, the VI-ASHP as a heating device is needed, which has an average COP of 3 and consumes 4394.6kWh of electricity during operation. The average EER of the heat pump for cooling is 6.4 whilst the annual electricity consumption for cooling is 355.2kWh. The electricity consumed by the water pumps of the system is 1290.4kWh. Hence, the annual total electricity consumption of the system is 6040.2kWh in total. The PV model can produce 216.2 kWh/m² annually. With 4 × 2 m² PV panels, the yearly electricity generation by solar energy is 1729.6kWh. According to the feed-in tariff of 0.75RMB/kWh in Shanxi, the served house can earn 1297.2RMB per year by transferring the generated electricity to the power grid. Equally, with this amount of earned money, the PV module can provide 1633kWh electricity to the system. The energy contribution by solar thermal energy, photovoltaic energy and electricity from the power grid is 74.6%, 6.9% and 18.5% respectively.

In regard to the economic performance, the initial capital cost of the novel solar heat pump system is 30290RMB, in which the most expensive component is the VI-ASHP accounting for nearly 34% of the total cost. Due to lower operational costs compared with the conventional coal-based system, the novel system has a cost payback period of around 6.52 years and a life-cycle net cost saving of nearly 56328.4RMB in Shanxi, thereby indicating the system is economically viable.

The proposed system is also environmentally friendly. While a conventional coal-based system for a standard rural house in northern China may use 5tons of anthracite coal each year and generate 33.7 kg of harmful dust, 12.1tons of CO₂, 372.2 kg of SO₂ and 186.1 kg of NO_x, the solar-assisted VI-ASHP system can operate without contaminant emission and save the above amount of anthracite coal by employing solar and electrical energy. Based on the performance of the demonstration system, it is anticipated that a village of 100 sets of installed capacity will save 496.3tons of coal per year. During the 25-year life span, the total carbon emission reduction is 30276.7tons.

In summary, the novel solar-assisted VI-ASHP system can significantly improve energy efficiency and reduce the energy consumption for space heating, cooling, and hot water supply. It is a promising approach to near-zero carbon emission from buildings. Although the system is demonstrated in northern China, it is expected to be applicable in other cold regions of the world.

CRedit authorship contribution statement

Yi Fan: Investigation, Methodology, Formal analysis, Writing - original draft. **Xudong Zhao:** Supervision, Conceptualization, Funding acquisition. **Jing Li:** Supervision, Conceptualization, Project administration. **Guiqiang Li:** Resources. **Steve Myers:** Writing - review & editing. **Yuanda Cheng:** Software. **Ali Badiei:** Writing - review & editing. **Min Yu:** Data curation. **Yousef Golizadeh Akhlaghi:** Resources. **Samson Shittu:** Validation. **Xiaoli Ma:** Writing - review & editing.


Declaration of Competing Interest

The authors declare that they have no known competing financial interests or personal relationships that could have appeared to influence the work reported in this paper.

Acknowledgment

The authors would like to acknowledge our appreciation for the financial support received from the following projects: 'A low carbon heating system for existing public buildings employing a highly innovative multiple-throughout-flowing micro-channel solar-panel-array and a novel mixed indoor/outdoor air source heat pump' funded by the UK BEIS.

References

 The corrections made in this section will be reviewed and approved by a journal production editor. The newly added/removed references and its citations will be reordered and rearranged by the production team.

- [1] Evans M., Yu S., Song B., Deng Q., Liu J., Delgado A. Building energy efficiency in rural China. *Energy Policy* 2014;64:243–251. doi:10.1016/j.enpol.2013.06.040.
- [2] Zhu Saihong Su. Shan L shuang. The strategy of rural residential thermal environment adjustment in cold areas (in Chinese). *Art Technol* 2016;29:306–307.
- [3] Shan M., Wang P., Li J., Yue G., Yang X. Energy and environment in Chinese rural buildings: Situations, challenges, and intervention strategies. *Build Environ* 2015;91:271–282. doi:10.1016/j.buildenv.2015.03.016.
- [4] Zhang X., Zhao X., Shen J., Hu X., Liu X., Xu J. Design, fabrication and experimental study of a solar photovoltaic/loop-heat-pipe based heat pump system. *Sol Energy* 2013;97:551–568. doi:10.1016/j.solener.2013.09.022.
- [5] Diao Y.H., Wang S., Zhao Y.H., Zhu T.T., Li C.Z., Li F.F. Experimental study of the heat transfer characteristics of a new-type flat micro-heat pipe thermal storage unit. *Appl Therm Eng* 2015;89:871–882. doi:10.1016/j.applthermaleng.2015.06.070.
- [6] Tosun M., Doğan B., Öztürk M.M., Erbay L.B. Integration of a mini-channel condenser into a household refrigerator with regard to accurate capillary tube length and refrigerant amount. *Int J Refrig* 2019;98:428–435. doi:10.1016/j.ijrefrig.2018.11.012.
- [7] Li G., Diallo T.M.O., Akhlaghi Y.G., Shittu S., Zhao X., Ma X., et al. Simulation and experiment on thermal performance of a micro-channel heat pipe under different evaporator temperatures and tilt angles. *Energy* 2019;179:549–557. doi:10.1016/j.energy.2019.05.040.
- [8] Deng Y., Wang W., Zhao Y., Yao L., Wang X. Experimental study of the performance for a novel kind of MHPA-FPC solar water heater. *Appl Energy* 2013;112:719–726. doi:10.1016/j.apenergy.2013.06.019.
- [9] Fan Y., Zhao X., Li G., Cheng Y., Zhou J., Yu M., et al. Analytical and experimental study of an innovative multiple-throughout-flowing micro-channel-panels-array for a solar-powered rural house space heating system. *Energy* 2019;171:566–580. doi:10.1016/j.energy.2019.01.049.

- [10] Sateikis I., Lynikiene S., Kavolelis B. Analysis of feasibility on heating single family houses in rural areas by using sun and wind energy. *Energy Build* 2006;38:695–700. doi:10.1016/j.enbuild.2005.11.003.
- [11] Huang J., Fan J., Furbo S. Feasibility study on solar district heating in China. *Renew Sustain Energy Rev* 2019;108:53–64. doi:10.1016/j.rser.2019.03.014.
- [12] Chen X., Qi C. Nonlinear neighbor embedding for single image super-resolution via kernel mapping. *Signal Process* 2014;94:6–22. doi:10.1016/j.sigpro.2013.06.016.
- [13] Gong G., Tang J., Lv D., Wang H. Research on frost formation in air source heat pump at cold-moist conditions in central-south China. *Appl Energy* 2013;102:571–581. doi:10.1016/j.apenergy.2012.08.001.
- [14] Yao Y., Jiang Y., Deng S., Ma Z. A study on the performance of the airside heat exchanger under frosting in an air source heat pump water heater/chiller unit. *Int J Heat Mass Transf* 2004;47:3745–3756. doi:10.1016/j.ijheatmasstransfer.2004.03.013.
- [15] Hakkaki-Fard A., Aidoun Z., Ouzzane M. Improving cold climate air-source heat pump performance with refrigerant mixtures. *Appl Therm Eng* 2015;78:695–703. doi:10.1016/j.applthermaleng.2014.11.036.
- [16] Shao S., Zhang H., You S., Zheng W., Jiang L. Thermal performance analysis of a new refrigerant-heated radiator coupled with air-source heat pump heating system. *Appl Energy* 2019;247:78–88. doi:10.1016/j.apenergy.2019.04.032.
- [17] Wang X., Hwang Y., Radermacher R. Two-stage heat pump system with vapor-injected scroll compressor using R410A as a refrigerant. *Int J Refrig* 2009;32:1442–1451. doi:10.1016/j.ijrefrig.2009.03.004.
- [18] Wang W., Li Y. Intermediate pressure optimization for two-stage air-source heat pump with flash tank cycle vapor injection via extremum seeking. *Appl Energy* 2019;238:612–626. doi:10.1016/j.apenergy.2019.01.083.
- [19] Xu X., Hwang Y., Radermacher R. Refrigerant injection for heat pumping/air conditioning systems: Literature review and challenges discussions. *Int J Refrig* 2011;34:402–415. doi:10.1016/j.ijrefrig.2010.09.015.
- [20] Cho H., Baek C., Park C., Kim Y. Performance evaluation of a two-stage CO₂ cycle with gas injection in the cooling mode operation. *Int J Refrig* 2009;32:40–46. doi:10.1016/j.ijrefrig.2008.07.008.
- [21] Dutta A.K., Yanagisawa T., Fukuta M. An investigation of the performance of a scroll compressor under liquid refrigerant injection. *Int J Refrig* 2001;24:577–587. doi:10.1016/S0140-7007(00)00041-4.
- [22] Fernández-Hernández Francisco, Fernández-Gutiérrez Alberto, Martínez-Almansa Juan José, del Pino C., Parras L. Flow patterns and heat transfer coefficients using a rotational diffuser coupled

- [23] Athienitis A.K., Chen T.Y. Experimental and theoretical investigation of floor heating with thermal storage. *ASHRAE Trans* 1993;99:1049–1057.
- [24] Karimi M.S., Fazelpour F., Rosen M.A., Shams M. Comparative study of solar-powered underfloor heating system performance in distinctive climates. *Renew Energy* 2019;130:524–535. doi:10.1016/j.renene.2018.06.074.
- [25] Inard C., Meslem A., Depecker P. Energy consumption and thermal comfort in dwelling-cells: A zonal-model approach. *Build Environ* 1998;33:279–291. doi:10.1016/S0360-1323(97)00074-7.
- [26] Karakoyun Yakup, Acikgoz Ozgen, Yumurtacı Zehra, Dalkilic Ahmet Selim An experimental investigation on heat transfer characteristics arising over an underfloor cooling system exposed to different radiant heating loads through walls. *Appl Therm Eng* 2020;164:114517. doi:10.1016/j.applthermaleng.2019.114517.
- [27] Chen J., Yu J. Energy and exergy analysis of a new direct-expansion solar assisted vapor injection heat pump cycle with subcooler for water heater. *Sol Energy* 2018;171:613–620. doi:10.1016/j.solener.2018.07.019.
- [28] Lu S., Liang R., Zhang J., Zhou C. Performance improvement of solar photovoltaic/thermal heat pump system in winter by employing vapor injection cycle. *Appl Therm Eng* 2019;155:135–146. doi:10.1016/j.applthermaleng.2019.03.038.
- [29] CHN_Shanxi.Taiyuan. 537720_CSWD. Weather Data n.d. <https://energyplus.net/>.
- [30] Xudong Z., Xiaoli M. *Advanced Energy Efficiency Technologies for Solar Heating, Cooling and Power Generation*: Springer; 2019.
- [31] Zhou J., Zhao X., Ma X., Du Z., Fan Y., Cheng Y., et al. Clear-days operational performance of a hybrid experimental space heating system employing the novel mini-channel solar thermal & PV/T panels and a heat pump. *Sol Energy* 2017;155:464–477. doi:10.1016/j.solener.2017.06.056.
- [32] Cho I.Y., Seo H.J., Kim D., Kim Y. Performance comparison between R410A and R32 multi-heat pumps with a sub-cooler vapor injection in the heating and cooling modes. *Energy* 2016;112:179–187. doi:10.1016/j.energy.2016.06.069.
- [33] The compressor products brochure provided by Emerson Electric Co. n.d. <https://climate.emerson.com/documents/谷轮涡旋-zw系列热泵专用压缩机产品手册-zw-compressor-catalogue-zh-cn-5407826.pdf>.
- [34] Hans L., Fritz S. *Heat Pump Technology*. Butterworth-Heinemann; 1981.
- [35] Bell D.A., Towler B.F., Fan M., Bell D.A., Towler B.F., Fan M. *The Nature of Coal. Coal Gasif. Its Appl.*, William Andrew Publishing 2011;1–15. doi:10.1016/B978-0-8155-2049-8.10001-4.
- [36] Zhang Q., Yi H., Yu Z., Gao J., Wang X., Lin H., et al. Energy-exergy analysis and energy efficiency improvement of coal-fired industrial boilers based on thermal test data. *Appl Therm Eng*

- [37] Zhang X., Shen J., Xu P., Zhao X., Xu Y. Socio-economic performance of a novel solar photovoltaic/loop-heat-pipe heat pump water heating system in three different climatic regions. *Appl Energy* 2014;135:20–34. doi:10.1016/j.apenergy.2014.08.074.
- [38] The feed-in tariff price for PV panel 2018. http://www.ndrc.gov.cn/xwzx/xwfb/201712/t20171222_871333.html.
- [39] Nottingham T, User NE. Wang , Zhangyuan (2012) Investigation of a novel façade-based solar loop heat pipe water heating system . PhD thesis , University of Nottingham . Investigation of a Novel Façade-Based Solar Loop Heat Pipe Water Heating System. 2012.
- [40] Kannan R., Leong K.C., Osman R., Ho H.K., Tso C.P. Life cycle assessment study of solar PV systems: An example of a 2.7 kWp distributed solar PV system in Singapore. *Sol Energy* 2006;80:555–563. doi:10.1016/j.solener.2005.04.008.
- [41] Taiyuan electricity price 2018. <http://www.sdfcxw.com/dianfei/lvliang.html>.
- [42] Anthracite coal price 2018. <https://coalpail.com/coal-forum/viewtopic.php?f=112&t=50084>.
- [43] The contaminants generated by per unit anthracite coal n.d. <https://www3.epa.gov/ttn/chief/ap42/ch01/final/c01s02.pdf>.
- [44] The development of 100 sets of the novel solar-powered systems 2017. <http://www.sxrtv.com/content/v/a/2017-2-6/1486379276435.shtml?from=timeline&isappinstalled=0>.

Highlights

- First time that mini-channel panels are combined with vapor injection heat pump.
- Both heating and cooling performances throughout the year are estimated.
- Technology demonstration with panels of 36 m² and heat pump of 40 kW has been done.
- The payback time of the novel system is about 6.52 years.
- The annual carbon emission is reduced by 12.1tons for a rural house in northern China.

Queries and Answers

Query: Your article is registered as belonging to the Special Issue/Collection entitled “ICAE2019”. If this is NOT correct and your article is a regular item or belongs to a different Special Issue please contact j.ramkumar@elsevier.com immediately prior to returning your corrections.

Answer: Yes

Query: Please note that as per standard style, a corresponding author footnote be provided for at least one author.

Please check and assign the corresponding author name and also provide a professional email for the author.

Answer: *Corresponding author (Xudong Zhao) . Tel.: +44-01482466684, Email: xudong.zhao@hull.ac.uk

** Corresponding author (Jing Li). Tel.: +44-01482463611, Email: jing.li@hull.ac.uk

Query: The author names have been tagged as given names and surnames (surnames are highlighted in teal color).

Please confirm if they have been identified correctly.

Answer: Yes

Query: Have we correctly interpreted the following funding source(s) and country names you cited in your article:

BEIS, United Kingdom? /

Answer: Yes